

Control Structures and Properties of Missile Seekers

R N Bhattacharya, Non-member

T V Rao, Non-member

S Sadhu, Non-member

T K Ghoshal, Non-member

Airborne (target) seekers are interesting control systems as they have to perform dynamic tracking with low (pointing) error, implicit rate extraction as well as disturbance rejection. After introducing the general concepts, several possible variants of guidance signal extraction configurations are presented and analyzed. A special configuration called loop decoupling, where introduction of a tuned minor loop may potentially annul the effect of disturbance, has been formulated and sensitivity of such systems to meaningful perturbations in decoupling loop parameters are investigated. Other configurations where improved disturbance rejection is achieved by suitable mixing of outputs are formulated and analyzed in a similar manner. It is shown that in some cases, a systematic trade-off is possible between rejection of disturbance from guidance signal and pointing error by imperfect decoupling. Exact and approximate relations for evolving rational design procedure have been derived. The relations have been illustrated with the help of a numerical example.

Keywords : Missile control; Seeker; Tracking; Filtering; Homing guidance

NOTATION

D_1	: platform rate disturbance
D_2	: gyro bias or noise
E_1	: pointing error
E_2	: velocity servo error
F	: actual transfer function of decoupling block
\tilde{F}	: transfer function that satisfies decoupling condition
G_1	: forward path transfer function
G_2	: frequency dependent component of the angle channel receiver and compensators
\tilde{G}_1	: closed loop stab loop transfer function
\tilde{G}_2	: observed transfer function
\hat{G}_2	: closed loop tracker transfer function
H_1	: rate gyro transfer function
H_2	: pre-filter block
K	: velocity constant of the track loop
L_1	: outer loop gain with inner loop open
S_1	: sensitivity function
δF	: perturbations in transfer function of decoupling block
λ	: sight line angle
$\dot{\lambda}$: sight line rate
$\hat{\lambda}$: observed sight line rate
θ	: inertial dish angle

INTRODUCTION

Recently there has been some renewed interest in airborne target trackers or seekers for anti-ballistic missile¹ duties and because novel types of inertial sensors² and powerful on board computers are available, leading to the possibility of next generation missile seekers.

Objective of this paper is to present simplified relations, which helps in option analysis, specification and design of seekers. The simplified analysis presented here have been validated by the first two authors who have designed, simulated, constructed and tested such seeker systems and seeker based guidance in real life situations.

Airborne and especially missile borne seekers have to perform a number of duties simultaneously like:

- tracking a fast moving target with low (pointing) error,
- extracting the inertial rotational rate of the line joining the missile and the target (another missile or an aircraft) - for use by the guidance system,
- minimizing the effect of disturbance of the rotational motion of the carrier (missile) on pointing error and the extracted inertial rate.

Apart from its military roles, missile based seekers are versatile control systems and are therefore of interest to control system practitioners as well as to the academics. Despite such interests, availability of literature on this subject had been rather scanty, possibly because of its primarily military use. Notable exceptions to this are Garnell and East³, Nesline and Zarchan⁴, and Gentile and Tutt⁵. The first two works assume respectively first order and second order approximate models of the seeker but carry out a fairly detailed analysis on the impact of seeker performance on accuracy of homing guidance. Both of these works however do not discuss the internals of the seeker servo, which is important to evolve a rational design methodology for conventional or improved seekers. A free gyroscope⁶ based

R N Bhattacharya is with DRDL, Kanchanbag, Hyderabad; T V Rao is with RCI, Vigyan Kancha, Hyderabad and S Sadhu and T K Ghoshal are with Electrical Engineering Department, Jadavpur University, Kolkata 700 032.

This paper, received on June 20, 2000, was presented and discussed in Semi Annual Paper Meeting held at Hyderabad on July 15, 2001.

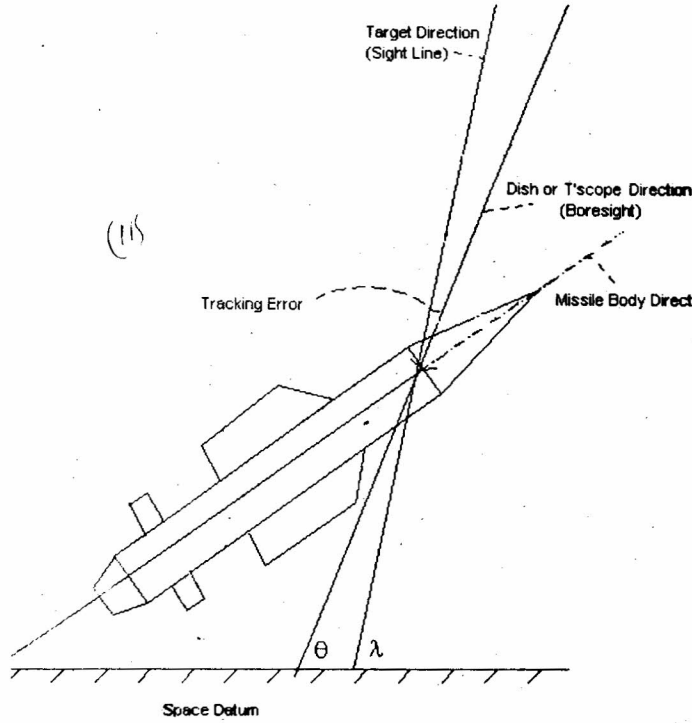


Figure 1 Basic geometry

design has been discussed by Merhav², which may not be extended for the rate gyro based designs, which are likely to be used in new generation seekers.

Most control system textbooks^{6,7} discuss ground based tracking systems like sun-trackers. Trackers for low earth orbiting satellites⁸ and for re-entering ballistic missiles⁹ have been discussed. However the important aspects of base motion disturbance rejection and implicit rate extraction duties are not covered in these works.

In the next section the concepts, structure and transfer functions of a simple rate gyro based seeker are briefly introduced. This plant, called the nominal plant, forms the base line for further discussions.

The performances and sensitivities of the so-named loop-decoupled seeker are described later and two 'non-invasive' signal extraction options are analyzed.

While the possibility of loop decoupled configuration had at least been mentioned in other^{3,5} literature, these non-invasive configurations, to the best of our knowledge, are appearing for the first time in this paper.

DESCRIPTION OF THE NOMINAL PLANT

Target tracking systems are used to track a moving target by orienting/moving its antenna or telescope (respectively a radar based or optical type) so as to always point towards the target. A target tracking system may be mounted on a stationary or slowly moving platform as in the case of command guided systems or may be placed in the missile as in the case of homing systems. Missile mounted target tracking systems are often called seekers.

A seeker attempts to align its electrical null axis or bore-sight in elevation and azimuth with the line of sight (LOS) *i.e.*, the line joining the seeker and the target. The basic geometry is shown in Figure 1.

The following kinematic and geometrical parameters are of interest in this context:

- Inertial reference line (say instantaneously aligned with the horizon).
- Missile attitude angle wrt. inertial axis.
- LOS (line of sight) joining the seeker and the target T.
- Boresight angle (angle between the reference line and telescope axis).
- Gimbal angle (angle between telescope and missile body).
- Pointing error or boresight error (difference between LOS and boresight angle).

A seeker has two identical servo-systems (one up down and the other left right) to align the telescope boresight with the target. The two servo systems will be similar for each of elevation axis

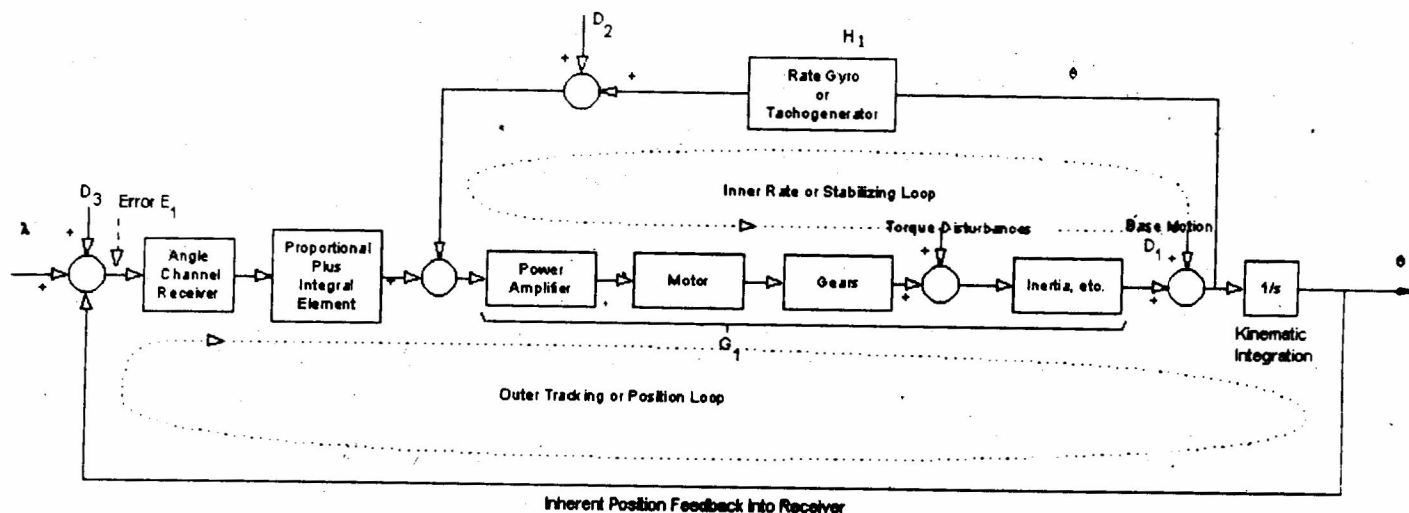


Figure 2 Block diagram of a seeker

and azimuth axis and only a single axis is discussed. The angular error detecting mechanism is either a radar receiver or an electro-optical signal processing system incorporating image-processing computer. The block diagram of a typical seeker is shown in Figure 2. The angle channel receiver produces a signal proportional to the misalignment between the target and its own bore-sight.

While for Radar's the angle channel error may be available either as an analog signal or sampled signal, the output for an imaging optical seeker is generally available as sampled (15 Hz to 60 Hz) signals. There may be additional processing delay in this type of seeker. While previous generation of air borne seekers employed free gyro, the more contemporary seekers are now based on rate gyros.

Each axis of a seeker system is generally organized with two loops called stabilization loop and the track loop.

The two loop combination is shown in Figure 3, where λ is the sight line angle, θ is the inertial dish angle, D_1 is the platform rate disturbance, D_2 is the gyro bias or noise and E_1 is the pointing error. The observer sight line rate is denoted as $\dot{\lambda}$.

The Stabilization Loop

The stabilization loop is the inner loop, which is basically a velocity servo comprising of a motor, drive gears and a rate gyro in the feedback path as shown in Figure 4. The forward path transfer function is G_1 and the block with transfer function H_1 represents the rate gyro. The pre-filter block H_2 is optional *i.e.*, it may have unity transfer function as is the case with most implementations. However for the time being, it is considered that $H_2 = H_1$ so as to make the transfer function of the servo system to be unity in ideal condition.

In order to find the steady state loop gain it is noted that steady state seldom occurs for a seeker during flight. However low frequency gain would be required for cases where the signal is slowly varying. For practical seekers it is noted that below a frequency of 1/r/s, it is reasonable to assume that the slope of the Bode plot is either zero (type zero system) or unity (for type 1 system). With this the low frequency gain of the stabilization loop is defined as

$$K_{v1} = \lim_{j\omega \rightarrow 1} |G_1(j\omega) H_1(j\omega)|$$

In cases where G_1 is chosen type-1 by integral action, it is noted that the velocity error constant automatically becomes the low frequency gain that is $K_{v1} = \lim_{s \rightarrow 1} sG_1(s) H_1(s)$.

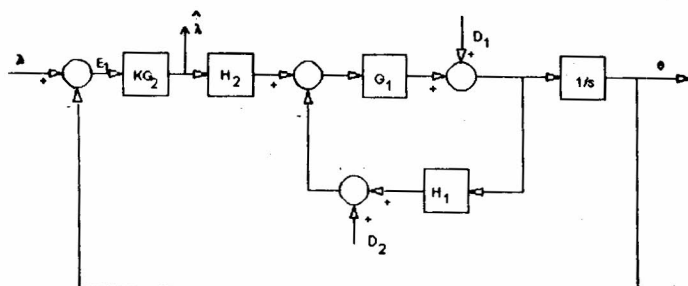


Figure 3 Stab loop and track loop

If the input to the velocity servo is zero, then under perfect stabilization condition the receiving surface will be inertially stabilized, *i.e.*, if it is aligned to a fixed star it will continue to do so even though its base *i.e.*, the missile may be having angular or translatory motions. By applying a voltage input to this perfect velocity servo the receiver surface may be made to move at a specified inertial rate. If, by some means, the boresight always points to the target, the input to the velocity servo must be the inertial sight line rate.

In a practical system, however, this will not be true due to bias and noise in the gyro (shown as D_2 in Figure 3) and imperfect isolation of base motion (shown as D_1 in Figure 3).

The closed loop transfer function of the stabilization loop is denoted as:

$$\tilde{G}_1 \triangleq \frac{\dot{\theta}}{\dot{\theta}_D} = \frac{G_1 H_2}{1 + G_1 H_1} \quad (1)$$

The corresponding sensitivity function¹⁰ is likewise defined as :

$$S_1 \triangleq \frac{H_1}{1 + G_1 H_1} \quad (2)$$

The gain cross over frequency of the stabilization loop alone is denoted by ω_1 , such that

$$|G_1(j\omega_1) H_1(j\omega_1)| = 1 \quad (3)$$

Base motion influences the stabilization system through friction, motor back emf and gearing system kinematics. It may be shown that the effect of base motion may be modeled adequately (for design purposes) by injecting the base motion velocity D_1 at the point shown in Figure 3 and Figure 4 and this is adopted by other workers³⁻⁵.

Velocity servo error E_2 due to D_1 may be estimated as

$$\frac{E_2}{D_1} = S_1 = \frac{H_1}{1 + G_1 H_1} \text{ volts} = \frac{H_1 / |H_1|}{1 + G_1 H_1} \text{ rad/s} \quad (4)$$

This is valid in the absence of track loop.

The amplifier gain and compensation for the stabilization (stab) loop are so chosen that the open loop transfer function has a high gain cross over frequency limited only by the gyro bandwidth, electrical time constant of the drive motor and the mechanical resonance frequency of the assembly⁶. Typical gain

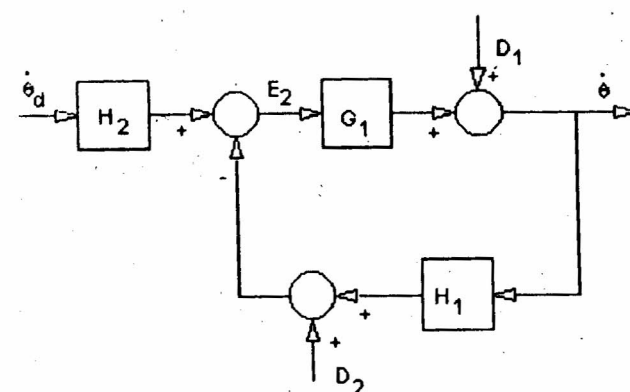


Figure 4 Stab loop

cross over frequency is about 15 Hz - 30 Hz. Attempt is made to make the gain cross over frequency at least a decade above the desired track loop bandwidth so that residual errors due to base motion may be easily filtered from the track loop.

The Track Loop

The track loop ensures that the sensing surface remains always pointed to the target. The boresight angle is obtained by kinematic integration of the boresight rate as shown in Figure 5 and Figure 3. In Figure 5, the stab loop is replaced by its equivalent closed loop transfer function.

The angle channel receiver measures the pointing error, which is amplified, compensated and thereafter used to drive the velocity servo. The track loop loop-transfer function is denoted as KG_2/s , where K is the velocity constant of the track loop and G_2 represents the frequency dependent components of the angle channel receiver (with associated delay and lag) and compensators. For this definition the stab loop is assumed to be ideal with unity closed loop gain.

The input point for the velocity servo is a convenient tapping point for sight line rate signal, to be used for guidance and can be called as observed sight line rate signal.

In ideal case, the velocity servo closed loop gain would be unity and with these assumptions, this approximate closed loop tracker transfer function of the track loop is denoted as :

$$\frac{\dot{\theta}}{\lambda} \approx \frac{KG_2/s}{1 + KG_2/s} \Delta \tilde{G}_2 \quad (5)$$

The gain cross over frequency of the track loop (with an ideal stab loop) alone is denoted by ω_2 .

The observer transfer function i.e, the relation of the target sight line rate and observed sight line rate also becomes

$$\frac{\dot{\lambda}}{\lambda} \approx \tilde{G}_2 \quad (6)$$

There would generally be a filter downstream of $\dot{\lambda}$ to attenuate signal beyond the track loop bandwidth, hence the observed sight line rate signals upto a frequency of ω_2 are of concern.

Interaction of the Two Loops

In a minor loop control system such as the tracker it is customary to design inner loop first keeping some margin for phase lag contribution from the outer loop. The contribution of the outer loop may be quantified by loop gain expression by breaking the inner loop.

$$L_1(s) = G_1 H_1 \left[1 + \frac{KG_2 H_2}{H_1 s} \right]$$

$$= G_1 H_1 \left[1 + \frac{KG_2}{s} \right] \text{ for } H_2 = H_1 \quad (7)$$

If the gain cross over frequencies of the outer and inner loops are not well separated, the phase contribution of $\frac{KG_2}{s}$ may be substantial at the inner loop gain crossover frequency ω_1 . However, it is derived from the disturbance isolation requirement that the gain crossover frequency ratio ω_1/ω_2 should be

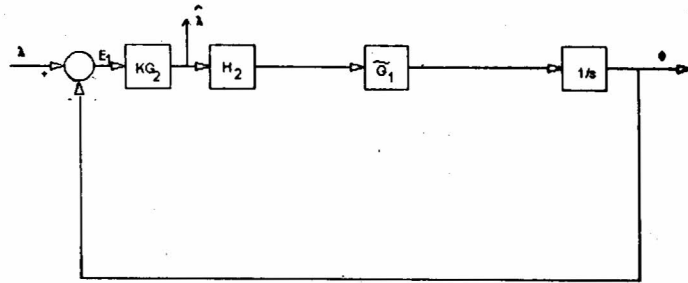


Figure 5 Track loop

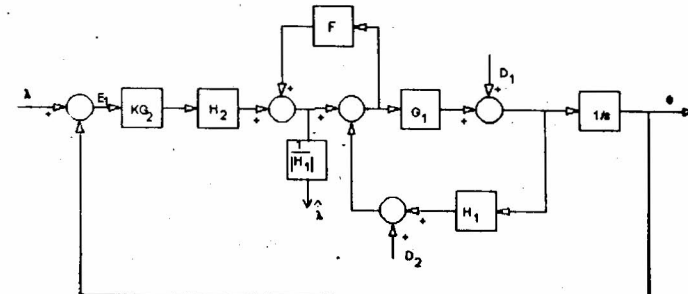


Figure 6 Loop decoupling

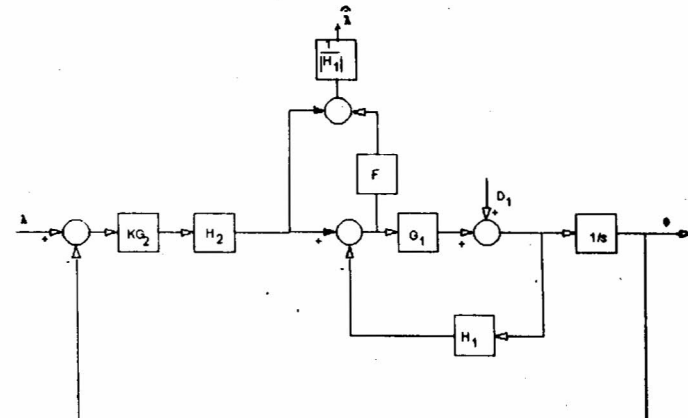


Figure 7 Non-invasive filter configuration

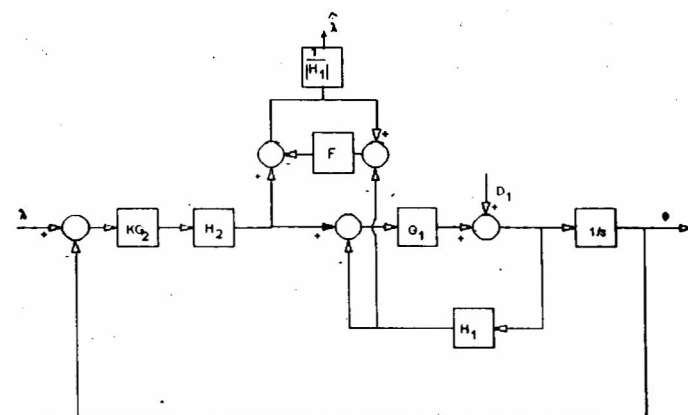


Figure 8 Rate base configuration

high and the phase angle contribution from outer loop was small.

With adequate separation, the magnitude contribution would be insignificant and it was assumed that gain crossover

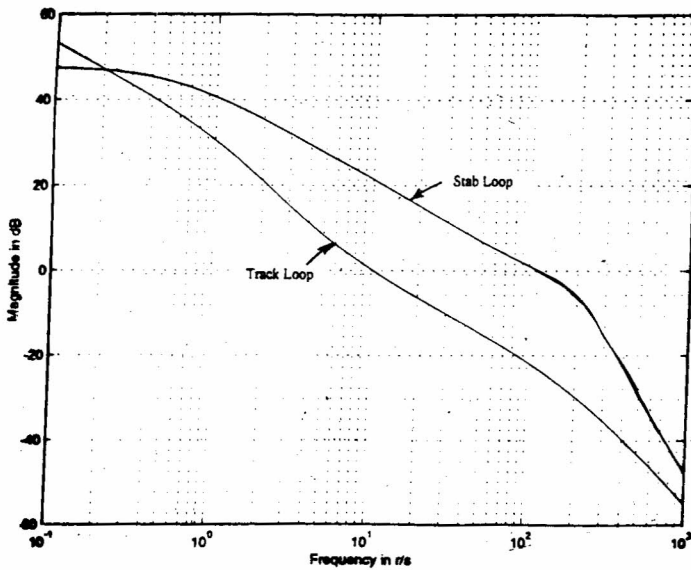


Figure 9 Bode plot of stab loop and track loop

frequency of the inner loop would remain relatively unaffected by the presence of the outer loop. Likewise the gain crossover frequency of the track loop would be more or less same as to the value obtained with ideal stab loop assumption.

Taking the effect of both loops, the closed loop tracker transfer function becomes

$$\frac{\dot{\theta}}{\lambda} = \frac{\tilde{G}_1 K G_2 / s}{1 + \frac{\tilde{G}_1 K G_2}{s}} \Delta \hat{G}_2 \quad (8)$$

It is noted that this would not be much different from the idealized transfer function \hat{G}_2 , as \tilde{G}_1 is nearly unity within the track loop bandwidth.

Typical Bode plots for track and stab loops are shown in Figure 9, using the plant transfer function given in the case study section.

Performance of the Basic Plant

Discussions would be limited on three performance items, (i) the observer transfer function, (ii) the (residual) error due to base motion in observed sight line rate and (iii) the pointing error.

Observer Transfer Function

The observer transfer function was derived as :

$$\frac{\dot{\lambda}}{\lambda} = \frac{K G_2 / s}{1 + \frac{\tilde{G}_1 K G_2}{s}} \quad (9)$$

Within track loop bandwidth, noting that $\tilde{G}_1 \approx 1$, the above expression may be approximated as

$$\frac{\dot{\lambda}}{\lambda} \approx \tilde{G}_2 \quad (10)$$

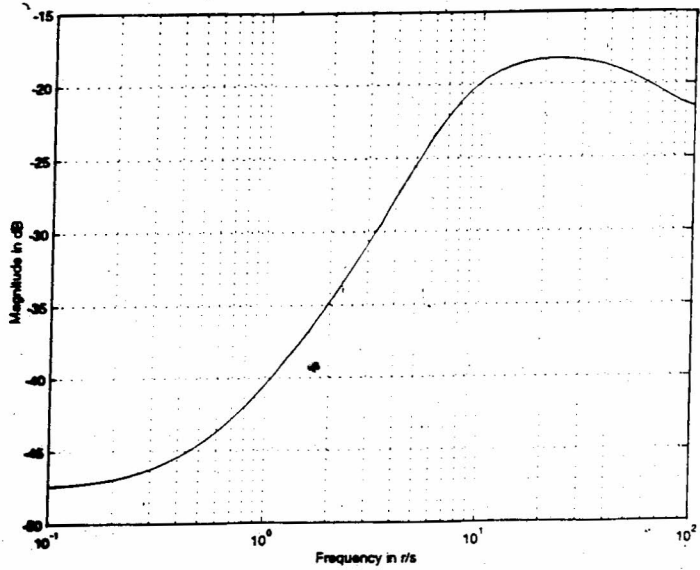


Figure 10 Frequency response of basic plant observed sight line rate to platform disturbance

Base Motion Rejection

The effect of platform disturbance on the observed sight line rate may be obtained as

$$\begin{aligned} \frac{\dot{\lambda}}{D_1} &= \frac{-K G_2 / s}{(1 + G_1 H_1) + K G_1 G_2 H_2 / s} \\ &= -\frac{\tilde{G}_1 K G_2 / s}{1 + \frac{\tilde{G}_1 K G_2}{s} \frac{1}{G_1 H}} = -\frac{1}{G_1 H} \times \hat{G}_2 \text{ for } H_2 = H_1 = H \end{aligned} \quad (11)$$

As before, within the track loop bandwidth, the above may be approximated as

$$\frac{\dot{\lambda}}{D_1} \approx \frac{1}{G_1 H} \quad (12)$$

The above transfer function suggests that the platform motion could be filtered mostly by the stabilization loop resulting in approximate transfer function of $1/G_1 H$. It may be shown that at the gain crossover frequency of the track loop, the disturbance isolation ratio would be around ω_1/ω_2 , which is typically 10 to 20 (20 dB to 30 dB). However, in reality, substantial amount of base motion may still appear in the observed signal because the base motion can be as high as ten times that of target sight line rate. Presence of base motion component may create instability in the guidance loop as described by Nesline and Zarchan⁴.

A typical Bode plot for the above transfer function is shown in Figure 10. The corresponding unit step response is shown in Figure 11.

Pointing Error

Because the seeker field of view is usually small, large pointing errors create a risk of losing the target. Pointing error or decentering error may occur due to target LOS rate ($\dot{\lambda}$) and also base motion (D_1). The following transfer function quantify such effects.

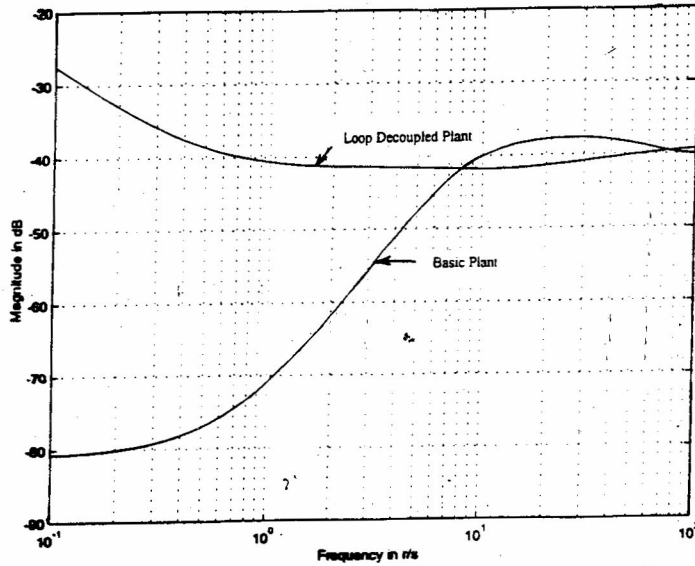


Figure 11 Frequency response of pointing error to platform disturbance for basic plant and loop decoupled plant

Pointing Error Due to Base Motion

$$\begin{aligned} \frac{E_1(s)}{D_1(s)} &= \frac{-1}{s(1 + G_1 H_1) + KG_1 G_2 H_2} \\ &= -\frac{1}{s} \times \frac{1}{1 + G_1 H_1} \times \frac{1}{1 + \frac{KG_2}{s} \times \tilde{G}_1} \\ &= -\frac{1}{G_1 HKG_2} \times \tilde{G}_1 \times \hat{G}_2 \end{aligned} \quad (13)$$

This expression is analyzed in different frequency regions.

- (i) At frequencies below track loop bandwidth transfer functions \tilde{G}_1 and \tilde{G}_2 may be approximated as unity, and the pointing error transfer function may be approximated as $-1/G_1 HKG_2$;
- (ii) At sufficiently low frequencies say around 1r/s, the open loop transfer function for the track loop is K and the same for stab loop may be approximated as K_{v_1} . This simplifies the above relation to $-1/(KK_{v_1})$; and
- (iii) At frequencies close to and above track loop bandwidth the pointing error transfer function may be approximated as $\frac{1}{s(1 + G_1 H_1)}$. This again has a value nearly equal to the constant value $\frac{1}{\omega_1}$.

The transient pointing error due to sharp base motion is generally dictated by the high frequency approximation as above. The last result indicates that such transient pointing error may be as high as D_1/ω_1 . This is not at all acceptable. Fortunately the base motion signal is necessarily band limited. One needs to choose the stab loop gain crossover frequency well above the base motion bandwidth.

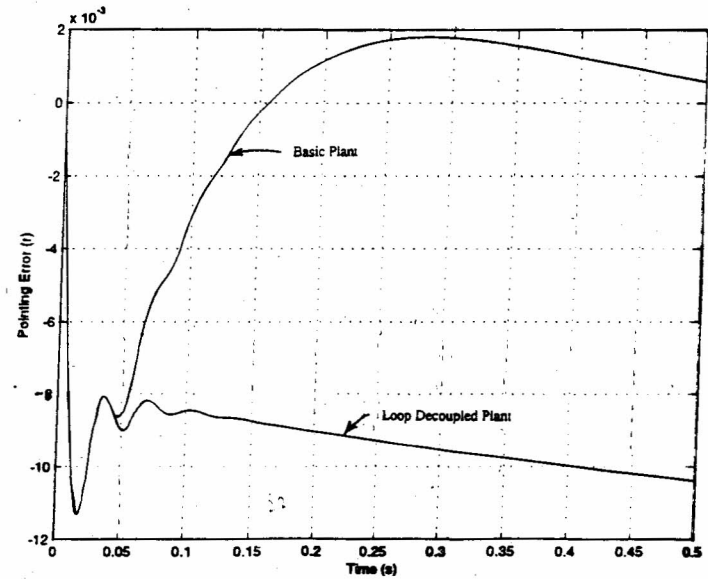


Figure 12 Basic plant and loop decoupled plant pointing error with 1 r/s base motion step

Typical Bode plot is shown in Figure 11. Typical step response is shown in Figure 12.

Pointing Error Due to Sight Line Rate

$$\frac{E_1(s)}{\lambda(s)} = \frac{1/s}{1 + \frac{G_1}{1 + G_1 H_1} \frac{KG_2}{s} H_2} \quad (14)$$

Within the track loop bandwidth the above expression may be approximated as $\frac{1}{s + KG_2}$ (assuming $H_1 = H_2$).

In steady state the pointing error due to unit sight line rate would therefore be $1/K$.

LOOP DECOUPLED SEEKER

Decoupling

It has been pointed earlier that filtering of platform rates from the observed sight line rate signal is of paramount importance for accuracy and stability of the guidance loop. Bandwidth of the sight line rate observer transfer function and isolation ratio are dictated by guidance considerations. For good isolation, a very large stabilization loop bandwidth is needed, which may not be feasible due to payload weight, cost and technology constraints. As suggested by Garnell³ connecting an additional loop¹¹, the platform rate contamination of the observed SLR signal may be, at least theoretically, eliminated. The present works have extended this concept to a configuration shown in Figure 6.

In this configuration, the point from where the observed sight line rate signal is tapped and also the gain adjustment block, F may be noted (Figure 6).

Considering the TF between the observed SLR and the platform disturbance input,

$$\frac{\hat{\lambda}}{D_1} = \left\{ \frac{FH_1 - \frac{KG_2 H_2}{s}}{1 + G_1 H_1 + F + \frac{KG_1 G_2 H_2}{s}} \right\} \frac{1}{|H|} \quad (15)$$

By setting $FH_1 = \frac{KG_2 H_2}{s}$, the numerator of the above TF becomes zero irrespective of the stab loop transfer function, implying that there will be no platform rate component on the observed SLR. This phenomenon is known as decoupling.

Further inspection of the decoupling condition indicates that this may be met by setting

$$H_2 = H_1 \text{ and } F = \frac{KG_2}{s}$$

This approach has several advantages over the one suggested in Garnell and East³ and Gentile and Tutt⁵ where $H_1 = 1$ and $F = KG_2 H_2/s$. As H_1 is the gyro transfer function, its bandwidth is typically 50 Hz. It is difficult to implement this in a digital computer with slow sampling rates. On the contrary H_2 can be implemented in the track loop using analog components. Again, G_2 contains the image processing (or signal processing depending upon IIR or radar seeker) transfer function,

which usually employs digital computer. So $F = \frac{KG_2}{s}$ can be better implemented by the same digital computer, which performs the image/signal processing function.

Another point to note is that the decoupling condition is independent of the stab loop transfer function. Thus nonlinearities like saturation and backlash (or even stick slip oscillation) will have no effect on the decoupling that is elimination of base motion signals from observed sight line rate.

The observer transfer function of the decoupled system becomes (assuming $H_1 = H_2 = H$)

$$\frac{\hat{\lambda}}{\lambda} = \frac{H_2}{|H|} \tilde{G}_2 \approx \tilde{G}_2 \quad (16)$$

The approximation would be valid within and slightly beyond the track loop bandwidth. This means that compared to the basic plant the filtering effects of the closed stab loop and its associated lag are both eliminated. This, however, is not a very significant advantage/disadvantage.

Pointing Error in Decoupled System

The relevant transfer function is

$$\frac{E_1(s)}{D_1(s)} = \frac{-1}{s(1 + G_1 H_1)} \quad (17)$$

A typical Bode plot is shown in Figure 11. It is that the high frequency performances of both the decoupled and ordinary systems are the same - implying that the transient error will be the same. This is justified intuitively.

At the low frequency end, around 1/r/s, the expression may be approximated as $1/(K_{v1})$. The error in long term may therefore be at least an order of magnitude higher than for the basic system. This provides an additional incentive to make the sight line bandwidth (SLBW) high and the low frequency gain of G_1 to be high.

For a type zero inner loop, the pointing error behaviour may be like an integrator at the very low frequency end. Where, the transient pointing error is ruling, this may not be a serious problem, otherwise, this factor alone may rule out the use of this scheme. A typical step response is shown in Figure 12.

During initial transients the frequency may be considered to be high with respect to the SLBW. As $|G_1 H_1| \ll 1$, during this period the input signal is simply integrated to a value close to $\int_0^{1/\omega_1} \omega_1 D_1 dt$ where ω_1 is the gain crossover frequency of the

stabilization loop. This part of the response is the same as that for undecoupled system. For a step input the above integration yields $|D_1|/BW_1$. Subsequently the frequency may be considered to be low and the integration proceeds with a gain of $1/(K_{v1})$. So a two-slope curve as shown in Figure 12 is expected. The above formula provides an easy way to estimate pointing errors.

It may be noted that the pointing error behaviour for decoupled system is solely dictated by the stab loop. Any saturation in the inner loop would aggravate the pointing error.

Sensitivity

It is conceivable that in practice exact satisfaction of the decoupling conditions is not possible due to uncertainties like time delay and non-linearities.

Let \tilde{F} be the transfer function that satisfies the decoupling condition. But the actual transfer function of the decoupling block be F , such that

$$F = \tilde{F} + \delta F \text{ where } |\delta F| \ll |\tilde{F}|$$

We now derive the relevant transfer function in presence of perturbation δF . $\frac{|\delta F|}{|\tilde{F}|}$ represents the per unit magnitude perturbations.

To take care of phase perturbation, we introduce $\tilde{F} + \delta F = \tilde{F} e^{-s\delta T}$, where δT is mismatch in time delay in implementing F .

$$\Rightarrow \frac{\delta F}{\tilde{F}} = e^{-s\delta T} - 1$$

It is to be noted, δT may also include the effect of ignoring fast poles/zeros in \tilde{F} .

Base Motion Isolation

$$\begin{aligned} \frac{\hat{\lambda}}{D_1} &= \frac{\frac{KG_2 H}{s} \left(\frac{\delta F}{\tilde{F}} \right)}{\frac{KG_2}{s} \left[\frac{\delta F}{\tilde{F}} + 1 + G_1 H \right] + 1 + G_1 H} \frac{1}{|H|} \\ &= \frac{KG_2 H}{s} \frac{1}{(1 + G_1 H) \left(1 + \frac{KG_2}{s} \right)} \frac{\delta F}{\tilde{F}} \frac{1}{|H|} \\ &\quad \left(\frac{\delta F}{\tilde{F}} \text{ factor in the denominator neglected} \right) \end{aligned}$$

$$= \tilde{G}_2 \times \frac{1}{G_1 H} \tilde{G}_1 \frac{\delta F}{\tilde{F}} \approx \frac{\delta F}{\tilde{F}} \times [\text{Effect in basic undecoupled system}] \quad (18)$$

It is therefore, noted that a 10% change in gain in implementing F would introduce a tenth of body rate signal that would have been obtained in a non-decoupled system. It is also noted that the effect is symmetric about $\delta F = 0$.

In order to limit the effect of phase shift error $\omega_2 T \ll \pi$ is maintained where ω_2 is the track loop gain crossover frequency. For a 10° phase mismatch about 16% platform rate component is expected compared to that for an undecoupled system as

$$|1 - e^{-s\delta T}|_{s=j\omega T} = |1 - 1 - 10^\circ| = 0.16$$

Theoretically speaking, the phase mismatch may amplify certain high frequency body rate component upto twice the value obtainable from undecoupled system. However high frequency signals are easily filtered without compromising track loop bandwidth.

Sensitivity to Pointing Error

$$\frac{E_1}{D_1} = - \frac{1 + F}{s \left(1 + F + G_1 H_1 + KG_1 \frac{G_2 H_2}{s} \right)} \quad (19)$$

Substituting $F = \tilde{F} + \delta F$, assuming $H_1 = H_2 = H$ and ignoring the δF term in the denominator

$$\begin{aligned} \frac{E_1}{D_1} &\approx \frac{1 + \tilde{F} + \delta F}{s(1 + \tilde{F})(1 + G_1 H)} = - \frac{1}{s} \left[\frac{1 + \frac{\delta F}{1 + \tilde{F}}}{1 + G_1 H} \right] \\ &= - \frac{1}{s} \left[\frac{1 + \frac{\delta F}{\tilde{F}} \frac{\tilde{F}}{1 + \tilde{F}}}{1 + G_1 H} \right] = - \frac{1}{s} \left[\frac{1 + \frac{\delta F}{\tilde{F}} \tilde{G}_2}{1 + G_1 H} \right] \\ &= \left(\frac{1}{s} \times \frac{1}{1 + G_1 H} \right) \left[1 + \frac{\delta F}{\tilde{F}} \tilde{G}_2 \right], \end{aligned} \quad (20)$$

The expression within the first bracket is the effect due to a perfectly decoupled system. The second term in the second bracket provides expression for additional pointing error due to detuning. From the above expression it is noted that the additional pointing error increases for positive magnitude change in δF and that for negative magnitude change in δF the additional pointing error decreases. Beyond the bandwidth of the track loop, such additional error would sharply decrease due to the closed loop transfer function for the track loop.

NON-INVASIVE DECOUPLING FILTERS

A side effect of the loop decoupling scheme discussed above is that the transfer function of the loops are altered, creating unacceptable situation in pointing error under certain conditions.

It is possible to isolate the base motion by non-invasive decoupling filter configurations. Non-invasiveness of these configurations lie in the fact that the tracking transfer function remains

the same as that for the basic system, in contrast to the loop decoupled configuration. Further, the pointing error is unaffected by such configuration augmentation. Two such non-invasive decoupling filter configurations, hereafter called as rate error based and rate based filters respectively, are shown in Figures 7 and 8. It may be shown that the effect of base motion disturbances on the observed sight line rate may be annulled in both the cases by appropriate choice of the filter block transfer functions.

Rate Error Based Configuration

For the rate error based configuration shown in Figure 7, the observed SLR is zero when

$$F = \frac{KG_2}{1 + \frac{KG_2}{s}} = \tilde{G}_2 \text{ and } H_1 = H_2 = H$$

The observer transfer function for this configuration is given by

$$\hat{\lambda} = \tilde{G}_2 \times \frac{H}{|H|} \approx \tilde{G}_2 \quad (21)$$

The sensitivity is given by

$$\hat{\lambda} = \frac{\delta F}{\tilde{F}} \frac{1}{G_1 H} \hat{G}_2 = \frac{\delta F}{\tilde{F}} \times [\text{Effect in basic undecoupled system}] \quad (22)$$

Rate-based Configuration

For the rate-based configuration shown in Figure 8, the observed SLR is zero when $F = KG_2/s$ and $H_1 = H_2 = H$.

The corresponding observer transfer function is

$$\hat{\lambda} = \frac{KG_2 H/s}{\left(1 + \frac{KG_2 H}{s} \right) |H|} = \tilde{G}_2 \frac{H}{|H|} \quad (23)$$

The sensitivity is given by

$$\begin{aligned} \hat{\lambda} &\approx \frac{\delta F}{\tilde{F}} \frac{1}{G_1 H} \hat{G}_2 \frac{1}{1 + \frac{KG_2}{s}} \\ &= \frac{\delta F}{\tilde{F}} \frac{1}{1 + \frac{KG_2}{s}} \times [\text{Effect in undecoupled system}] \end{aligned} \quad (24)$$

MODEL FOR CASE STUDY

A nominal plant has been studied to validate the discussion made earlier. The transfer functions of the various components have been assumed to be as follows :

$$G_1 = \frac{4}{1 + s/25} \frac{60(1 + s/30)}{1 + s/0.5}$$

$$\text{Gyro transfer function} = \frac{200^2}{s^2 + 200s + 200^2}$$

$$KG_2 = \frac{9.322(s + 5)}{s(s + 1)(1 + 0.005s)}$$

A delay of 20 ms has been assumed in the track loop.

The stab loop gain crossover frequency is at 100 rad/s and the track loop is at 10.26 rad/s.

DISCUSSIONS AND CONCLUSIONS

- (i) In this paper, only two non-invasive filtering configurations have been provided. Several other options are possible at least one of which has advantages in practical realization. In fact, due to space limitations implementation options were not discussed. Other possible configurations include Kalman filter - like external loop.
- (ii) It would be evident that the non-invasive configurations are superior to loop decoupled configuration because there is no adverse pointing error effect in the former.
- (iii) From the pointing error response example, it may appear that as the transient pointing error for loop decoupled, and other configurations are same, the pointing error could not be a selection criteria. This is not true because, in Figure 12 a step body rate has been used whereas in practice the most severe type of disturbance could be a first order filtered step. Such inputs reduce the transient error by a factor of five and the long term pointing error rates.
- (iv) The two non-invasive configurations actually have same sensitivity though equation (22) and equation (24) look quite different. It must be noted that in the rate-based configuration, the filter transfer function F needs to implement the closed loop transfer function. As such

$$\delta F = \frac{\delta [KG(s)/s]}{1 + KG(s)/s}$$

- (v) It is hoped that the foregoing analysis and discussions would enable a designer to quickly carry out a rough design and perform analysis of implementation options.

ACKNOWLEDGEMENTS

The authors wish to thank colleagues of Jadavpur University Prof Kalyankumar Datta, Prof Shyamal Goswami, Prof Samar Bhattacharyya for initial modelling and constructive criticisms, and Dr S K Chaudhuri, RCI, for hardware-in-loop simulations for verifying the theoretical results. They also thank Directors of RCI, DRDL, and ADA of DRDO for funding the initial projects and supporting one of the authors.

REFERENCES

1. 'Ballistic Missile Defense, Special Report.' *IEEE Spectrum*, September, 1997.
2. S Merhav. 'Aerospace Sensor Systems and Applications.' *Springer*, 1996.
3. P Garnell and D J East. 'Guided Weapon Control Systems.' *Pergamon Press*, Elmsford, N Y, 1977.
4. F W Nesline and P Zarchan. 'Line of Sight Reconstruction for Faster Homing Guidance.' *Journal of Guidance*, February 1985.
5. F Gentile and G Tutt. 'Target Track and Stabilization for Manportable Direct Fire Missiles. Final Report, US Army Missile, R & D Command Redstone Arsenal, Alabama, vol 1, November 1981.
6. E O Doebelin. 'Control System Principles and Designs.' *John Wiley and Sons*, 1990.
7. B C Kuo. 'Automatic Control Systems.' *Prentice Hall of India Pvt Ltd*, New Delhi, 1995.
8. W Gawronski and J A Mellstrom. 'Antenna Servo Design for Tracking Low-Earth Orbiting Satellites.' *Journal of Control, Guidance and Dynamics*, vol 17, no 6, 1994, p 1170.
9. G Biernson. 'Optimal Radar Tracking Systems.' *John Wiley and Sons, Inc*, 1990.
10. D E Davison, P T Kabamba and S M Meerkov. 'Limitations of Disturbance Rejection in Feedback Systems with Finite Bandwidth.' *IEEE Transactions on Automatic Control*, vol 44, June 1999, p 1132.
11. W W Willman. 'Effect of Seeker Scale Factor Uncertainty on Optimal Guidance.' *Journal of Control Guidance and Dynamics*, vol 11, no 3, May-June 1988, p 199.
12. G Das. 'Structured Methodology for Aerospace FCS Design.' *PhD Thesis*, Jadavpur University, 1998.